

Role of van der Waals bonding in the layered oxide V_2O_5 : First-principles density-functional calculations

Elisa Londero^{1,2} and Elsebeth Schröder^{1,*}¹*Microtechnology and Nanoscience, MC2, Chalmers University of Technology, SE-412 96 Göteborg, Sweden*²*Applied Physics, Chalmers University of Technology, SE-412 96 Göteborg, Sweden*

(Received 5 June 2010; published 23 August 2010)

Sparse matter is characterized by regions with low electron density and its understanding calls for methods to accurately calculate both the van der Waals (vdW) interactions and other bonding. Here we present a first-principles density-functional theory (DFT) study of a layered oxide (V_2O_5) bulk structure which shows charge voids in between the layers and we highlight the role of the vdW forces in building up material cohesion. The result of previous first-principles studies involving semilocal approximations to the exchange-correlation functional in DFT gave results in good agreement with experiments for the two in-plane lattice parameters of the unit cell but overestimated the parameter for the stacking direction. To recover the third parameter we include the nonlocal (dispersive) vdW interactions through the vdW-DF method [M. Dion, H. Rydberg, E. Schröder, D. C. Langreth, and B. I. Lundqvist, *Phys. Rev. Lett.* **92**, 246401 (2004)] testing also various choices of exchange forms. We find that the transferable first-principles vdW-DF calculations stabilizes the bulk structure. The vdW-DF method gives results in fairly good agreement with experiments for all three lattice parameters.

DOI: [10.1103/PhysRevB.82.054116](https://doi.org/10.1103/PhysRevB.82.054116)

PACS number(s): 31.15.E-, 71.15.Mb, 71.15.Nc, 61.50.Lt

I. INTRODUCTION

Vanadium is one of the most abundant metals on earth and it is found in about 150 different minerals. Catalysts based on vanadium oxides are widely used in the production of chemicals and in the reduction in environmental pollution, in particular, the vanadium pentoxide (V_2O_5) form is extensively used.¹ In recent years V_2O_5 has also been used with intercalating Li ions for high-capacity solid-state batteries.²⁻⁵ The applied research and industrial focus on catalysis and batteries involving V_2O_5 has led to a substantial amount of atomic-scale theory studies focusing on the V_2O_5 bulk⁵⁻¹² and its surfaces.¹²⁻¹⁶

The bulk of V_2O_5 has a stacked structure. Previous atomic-scale calculations that were based on density-functional theory (DFT) with the popular semilocal generalized gradient approximations (GGAs) have often failed in arriving at the experimentally known value of the lattice parameter in the stacking direction of the layers.⁸⁻¹³ This is believed to happen because GGA does not describe the van der Waals (vdW) forces,¹⁷ and because these are expected to play an important role in binding the layers in V_2O_5 bulk.¹² In several GGA-based V_2O_5 surface or vacancy studies this deficiency of GGA was either ignored or worked around by imposing the experimentally obtained lattice parameter or unit-cell volume. Other groups have employed the semi-empirical method DFT-D (Ref. 18) for adding the vdW forces.¹⁹

In this paper we use the first-principles vdW density-functional approach, vdW-DF,^{20,21} to determine the V_2O_5 bulk structure. We find that the vdW forces are indeed important for binding the structure, and we analyze the binding within and mainly between the layers. We here focus solely on the common α - V_2O_5 bulk structure and ignore the more exotic γ - V_2O_5 structure.^{6,10}

The vdW-DF method has a different philosophy and aim and some advantages over the DFT-D method. The DFT-D

approach to include the vdW forces is an atom-centered pair-potentials method. The vdW-DF method is directly based on the electron response. The vdW-DF method correctly describes the interaction as arising in the tails of the electron distribution, not at the atomic centers. Unlike DFT-D, vdW-DF provides a framework which is well suited to include effects of image planes.²² The DFT-D omission of image planes can result in inconsistencies of the description across a range of distances.²³ This effect could be important in materials such as V_2O_5 where the corrugation is large, and where as a result both relatively small and larger distances contribute to the vdW interaction simultaneously.

The outline is as follows. In Sec. II we describe the structure of V_2O_5 as known from experiments. In Sec. III we describe the computational methods used, both the self-consistent (sc) GGA calculations that provide the electron density, and the postprocess procedure that takes this density as input for obtaining the vdW contribution. Section IV is devoted to the discussion of our results and Sec. V includes a summary.

II. MATERIAL STRUCTURE

The (α -) V_2O_5 bulk has orthorhombic symmetry and a layered structure: each vanadium atom is connected to five oxygen atoms to create pyramids that share their corners in building a double chain. The chains are connected along the edges to form layers that are then stacked to form the bulk structure (Fig. 1).

There are three structurally different oxygen atoms in each layer. One is coordinated to one vanadium atom, the second is found in a bridging position, and the third has a threefold-coordinated position. The binding of the atoms inside a layer is strong whereas the interactions that keep the layers stacked are weaker, resulting in V_2O_5 being easily cleaved.

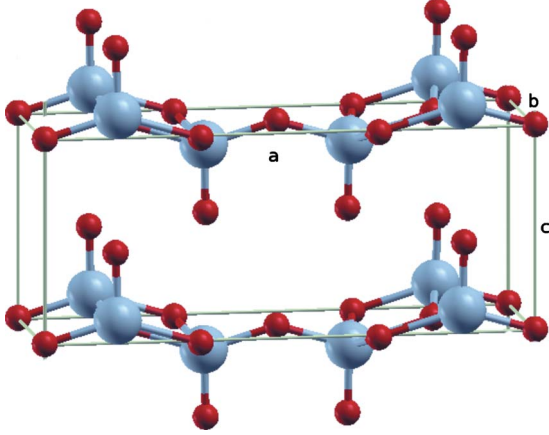


FIG. 1. (Color online) The structure of V_2O_5 bulk (α phase). The box shows the primitive unit cell that contains 2 f.u. The 14 atoms of the unit cell are shown, as well as a number of the atoms of the neighboring unit cells. V atoms are represented by large spheres and O atoms by small spheres. The labels a , b , and c indicate the vectors that span the orthorhombic unit cell. The cleavage plane is perpendicular to the c direction. Figure created using XCRYSDEN (Ref. 24).

III. COMPUTATIONAL METHODS

For determining the bulk structure of V_2O_5 we use the first-principles nonlocal functional vdW-DF within DFT.²⁰ We calculate the vdW-DF energies in a post-GGA procedure. This is reasonable since the differences in the resulting atomic positions and total energies to those of a fully self-consistent vdW-DF calculation have been shown to be negligible.²¹

The main interest here is on determining the optimal interlayer spacing in V_2O_5 (which is the same as the unit-cell side length c , Fig. 1) and the binding energy, defined as the energy gained by stacking layers of V_2O_5 . We calculate the vdW-DF total energy $E^{\text{vdW-DF}}$ for a number of values of c and find the minimum of the energy curve. For each point on the energy curve the procedure requires first a sc-GGA calculation, from which the GGA-based total energy $E_{\text{tot}}^{\text{GGA}}$ and the sc-GGA electron density n are evaluated. Then n is used for evaluating the long-range correlation contribution arising from the vdW interactions, E_c^{nl} . Following the systematic procedure described in more detail in several other publications,^{22,25,26} and summarized below, we combine the sc-GGA and nonlocal results to obtain $E^{\text{vdW-DF}}$.

This section contains three parts explaining the computational methods used. The first part deals with the sc-GGA calculations used as a basis for obtaining n and some terms of the energy $E^{\text{vdW-DF}}$. The second part contains a short summary of the scheme used for the calculation of E_c^{nl} and the vdW-DF total energy $E^{\text{vdW-DF}}$, and the third part briefly explains the effect and importance of choice of exchange functional for use in vdW-DF.

A. sc-GGA calculations

The sc-GGA calculations are carried out using the plane-wave code²⁷ DACAPO with ultrasoft pseudopotentials (US-

PPs). We describe V_2O_5 by an orthorhombic unit cell containing 2 formula units (f.u.), periodically repeated in all directions. The energy cutoff for the expansion of the wave functions is set to 500 eV. The sc-GGA calculations are carried out using the Perdew, Burke, and Ernzerhof (PBE) (Ref. 28) form of the GGA for the exchange and correlation functional. The fast Fourier transform (FFT) grid is chosen such as to have a distance less than 0.12 Å between nearest-neighbor grid points. The choice of this relatively dense electron-density grid is important for the quality of the subsequent evaluation of the nonlocal correlation contribution. The Brillouin zone of the unit cell is sampled according to the Monkhorst-Pack scheme by means of a $2 \times 4 \times 4$ k -point sampling.

Our results are converged with respect to the wavefunction cutoff, the number of k points needed, and a number of code-internal parameters. By lowering the number of k points in the c direction we notice an insignificant (~ 0.001 eV) change in the minimum value of the sc-GGA total-energy curve.

Since the intraplanar bonds have an ionic and partly covalent nature²⁹ we assume the layers to remain rigid when changing the interlayer spacing c . This means that the atoms are kept fixed in their positions (found at the PBE binding distance) relative to the layer as the distance between the layers is changed with fixed atom-atom distances within the layers. By analyzing the residual Hellmann-Feynman forces on the atoms, calculated from the GGA-based electron density, we find that this is a reasonable approximation.

In this paper we define the binding energy E_b of V_2O_5 to be the energy gained by moving together isolated layers of V_2O_5 to form the bulk structure. Each unit cell in the bulk contains 2 f.u. in one layer, periodically repeated, and the reference (layers far apart) calculation is carried out with vacuum added on both sides of the layer. The reference calculation is for a unit cell that has the c direction side length four times that of the original unit cell, periodically repeated in all directions.³⁰ We use the same reference unit cell for the nonlocal correlation (E_c^{nl}) reference calculations and this imposes additional constraints on the construction of the reference unit cell, as described further below.

To supplement our analysis of the electron density with a better description of the core electrons we carry out a set of additional GGA calculations using the all-electron DFT code GPAW (Ref. 31) that is based on projector augmented waves³² (PAWs). In these calculations we use settings of computational parameters as close as possible to the parameters we use in DACAPO.

B. vdW density functional

We use the vdW-DF scheme to include the vdW interactions in a systematic manner. The correlation energy E_c is split³³ into a nearly local part E_c^0 and a part that includes the most nonlocal interactions E_c^{nl} ,

$$E_c = E_c^0 + E_c^{\text{nl}}. \quad (1)$$

The splitting of the correlation contributions makes it possible to employ different approximations for each term. In a

homogeneous system the term E_c^0 is the correlation E_c^{LDA} obtained from the local-density approximation (LDA), and in general²⁰ we approximate E_c^0 by E_c^{LDA} . The E_c^{nl} vanishes for a homogeneous system. It describes the coupling through the electrodynamic field, the dispersion interaction. The difference in E_c^{nl} contributions provides a description of the interaction which acts across large distances. The difference is not much influenced by large variations in the electron density. Rather, it is susceptible to the more coarse-grained response of the environment. The form of E_c^{nl} is derived in Ref. 20 and is

$$E_c^{\text{nl}}[n] = \frac{1}{2} \int \int d\mathbf{r} d\mathbf{r}' n(\mathbf{r}) \phi(\mathbf{r}, \mathbf{r}') n(\mathbf{r}'), \quad (2)$$

where ϕ is a kernel, explicitly stated in Ref. 20.

The electron density n that enters Eq. (2) is taken from the sc-GGA calculations and is described on a grid (the FFT grid of the sc-GGA calculation). Our code for evaluating E_c^{nl} is not periodic. However, as described in detail in Refs. 22, 30, and 34, the natural periodicity within the bulk unit cell is easily represented by explicitly including a number of the periodic images of the unit cell, with the nearby grid points carefully described and the grid points far away only described via a coarse version of the grid.

Similar to the energy contributions from the sc-GGA calculations the term E_c^{nl} must be evaluated relative to a reference calculation with the V_2O_5 layers ‘‘far apart.’’ As described above, this is here achieved with a unit cell four times the original unit cell in the c direction, with the V_2O_5 layer placed close to the middle of the unit cell. For this reference calculation of E_c^{nl} no periodicity in the c direction is assumed. The layer must be placed such that locally, with respect to the (FFT) grid points on which n is described, the nuclei maintain the same positions in the bulk and the reference calculation. This means that the (FFT) grid must be chosen such that the bulk and the reference calculations have the exact same grid point separation; in this study we need precisely four times the number of FFT points in the reference calculation compared to the original bulk calculation.

The combination of correlation terms in Eq. (1) avoids double counting of correlation contributions. Using the correlation energy E_c from Eq. (1) the total energy in the vdW-DF scheme is

$$E^{\text{vdW-DF}} = E_{\text{tot}}^{\text{GGA}} - E_c^{\text{GGA}} + E_c^{\text{LDA}} + E_c^{\text{nl}}, \quad (3)$$

where $E_{\text{tot}}^{\text{GGA}}$ is the total energy from the sc-GGA calculation and E_c^{GGA} and E_c^{LDA} the GGA respective LDA correlation calculated from the sc-GGA electron density n . The layer binding energy E_b (per unit cell) we define as the energy gained by moving the layers in V_2O_5 together accordionlike,³⁰

$$E_b = -(E_{\text{bulk}}^{\text{vdW-DF}} - E_{\text{ref}}^{\text{vdW-DF}}). \quad (4)$$

C. Exchange functionals

With every choice of approximation for correlation functional comes a need for choosing a suitable exchange func-

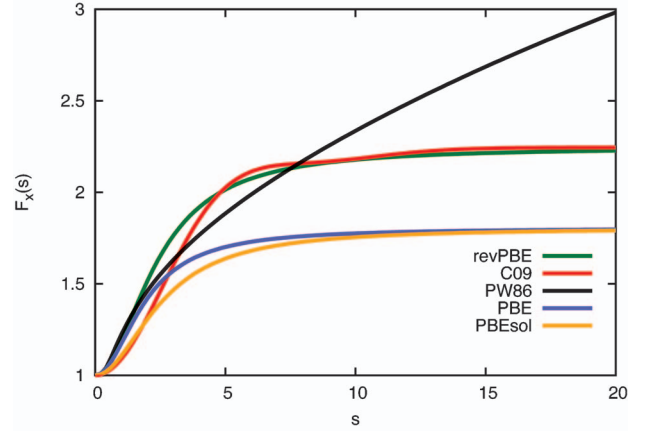


FIG. 2. (Color) Exchange functional enhancement factors F_x as functions of the reduced density gradient $s \sim |\nabla n|/n^{4/3}$. Shown are the exchange forms used here.

tional. In previous work we have chosen to combine the correlation E_c of Eq. (1) with the exchange from the GGA functional revPBE.³⁵ This choice has been the default for some time because calculations^{20,36} have shown that revPBE_x (by subscript x we denote the exchange part of the density functionals) does not give rise to spurious binding. This choice of revPBE_x is thus conservative in that it ensures that all the improvement in binding compared to GGA calculations comes from the improvement in correlation, Eq. (1).

However, it has also been shown that revPBE_x is overly repulsive in the binding region of many vdW-bonded systems.³⁷ In the present paper our aim is to study the binding of the layers of V_2O_5 by qualitatively examining the improvement in binding in the vdW-DF calculations over the usual GGA calculations. We do not here aim for a ‘‘perfect’’ description of the binding in the sense of best possible numerical fit to experiment. Rather, by showing the results of using a few choices of sound exchange functionals, we illustrate the sensitivity to those choices and find the range of values of c and E_b within which we expect the physical values to be. Two forthcoming publications³⁸ address and discuss choices of exchange functionals with vdW-DF in extended (layered) systems. In the present presentation of V_2O_5 binding we pick three promising candidates for exchange to use with vdW-DF, besides the well known PBE_x and revPBE_x functionals. These are PBEsol_x (Ref. 39), C09_x (Ref. 40), and PW86_x (Ref. 41).

GGA exchange may be described by the enhancement over LDA exchange in terms of the enhancement factor F_x ,

$$E_x = \int d\mathbf{r} n(\mathbf{r}) \epsilon_x^{\text{LDA}}[n(\mathbf{r})] F_x[s(\mathbf{r})], \quad (5)$$

where $\epsilon_x^{\text{LDA}} = -c_x n^{1/3}$ with $c_x = 3^{4/3}/(4\pi^{1/3})$ is the LDA exchange energy density and $s = c_s |\nabla n|/n^{4/3}$ with $c_s = 1/(2\pi^{2/3}3^{1/3})$ is the reduced electron-density gradient. The $F_x(s)$ curves for the exchange forms considered here are shown in Fig. 2 for a range of s values.

Dense materials have significant electron densities in most regions of the material and relevant values of s for

TABLE I. Equilibrium lattice parameters (a , b , and c) and interlayer binding energy per unit cell (E_b). Numbers in parenthesis are obtained by PW91 calculations and used in the calculations indicated. For the vdW-DF calculations the exchange functional used is shown explicitly with subscript x denoting the exchange part of the exchange-correlation functional. The LDA results are shown for comparison only and should not be considered an option for a physics-based account.

	a (Å)	b (Å)	c (Å)	E_b (eV)	C_{33} (GPa)
This work					
PBE with USPP	11.52	3.57	4.87	0.18	24
PBE with PAW ^a	(11.55)	(3.58)	4.89	0.21	21
vdW-DF, revPBE _{x} ^b	(11.55)	(3.58)	4.72	0.84	23
vdW-DF, revPBE _{x}	(11.55)	(3.58)	4.72	0.86	22
vdW-DF, PBE _{x}	(11.55)	(3.58)	4.46	1.28	57
vdW-DF, PBEsol _{x}	(11.55)	(3.58)	4.28	1.48	55
vdW-DF, PW86 _{x}	(11.55)	(3.58)	4.46	1.19	61
vdW-DF, C09 _{x}	(11.55)	(3.58)	4.28	1.10	58
LDA	(11.55)	(3.58)	4.18	1.07	49
Comparison					
PW91 with PAW ^c	11.55	3.58	4.84	0.25	
Experiment ^d	11.512	3.564	4.368		
Experiment ^e	11.508	3.559	4.367		

^aUsing the DFT code GPAW.

^brevPBE _{x} using the DACAPO code (please see main text).

^cReference 12, E_b is here estimated as the cleavage energy, calculated from the given surface energy of truncated surfaces: 0.048 J/m².

^dReference 44.

^eReference 4, powder of V₂O₅ (~420 nm crystals).

those systems lie mainly in the range⁴² $0 < s < 3$. For sparse materials, with regions of very low electron densities, values of $s > 3$ also play a role and cannot be ignored.⁴³ As is clear from Fig. 2 the various forms of exchange give different contributions at large values of s and the choice of exchange form is therefore more important for sparse than for dense matter.

In practice we include a particular exchange functional into the vdW-DF by subtracting the PBE _{x} energy contribution E_x^{PBE} from the total energy $E_{\text{tot}}^{\text{GGA}}$ of the sc-GGA calculations (because the sc-GGA calculations are carried out with the PBE form of GGA) and adding the value of the relevant exchange energy, calculated from the sc-GGA electron density n .

IV. RESULTS AND DISCUSSION

A number of previous DFT studies of the V₂O₅ bulk system have used GGA calculations for obtaining the lattice constants of the orthorhombic unit cell.^{5–12} The in-plane lattice parameters, in the present paper called a and b (but in parts of the literature called a and c), are found to be close to the experimental values. Table I lists for comparison the results of two experiments as well as the GGA results of Ref. 12. The interplane binding distance is the same as the third lattice parameter (here c , in parts of the literature b). For c a number of groups have found significantly larger values than

the experimental value.^{8–13} Ganduglia-Pirovano and Sauer¹² carried out GGA calculations using PW91 (Ref. 45) with PAW, emphasizing convergence and accuracy. This resulted in a c lattice constant even further away from the experimental value than the values from previous GGA calculations.

The deficiency in the description of the binding from GGA calculations has been attributed to the presence of vdW interactions between the V₂O₅ layers.¹² It is well known that GGA does not adequately describe vdW interactions,³³ thus if the layers of V₂O₅ are mostly bound to each other by vdW forces it is not surprising that GGA calculations do not give physically reasonable results. In the following we report our results from GGA calculations, from vdW-DF calculations, and discuss the effect of exchange and the binding character of V₂O₅.

A. GGA results

Exploring the V₂O₅ bulk system first with the (DACAPO-based) sc-GGA calculations we find, similar to the studies mentioned above, values of the a and b lattice constants in good agreement with experiment and a value for c about 11% too large when compared to experiment (Table I). The PBE total-energy curve is shallow in the c direction. In order to determine the minimum with any reasonable accuracy we first find the approximate minimum and then evaluate the total energy at 125 points in (a, b, c) parameter space in a small region around the approximate minimum. A three-

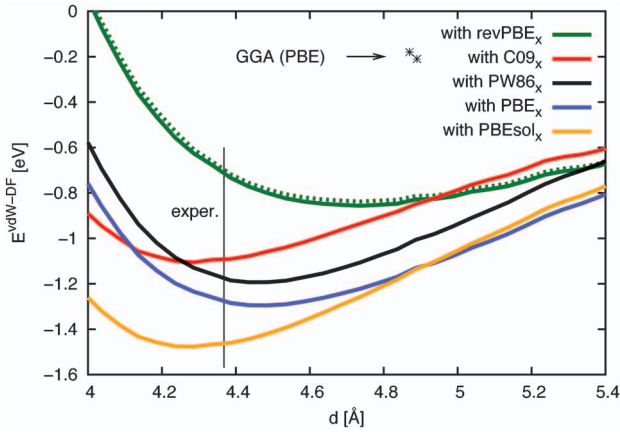


FIG. 3. (Color) $E^{\text{vdW-DF}}$ using various exchange choices. For revPBE_x we plot both the result of using the exchange energy provided directly by DACAPO (dashed line) and using our external implementation (solid lines). The two stars indicate the optimal points of our two PBE-based GGA calculations and the vertical line the experimentally found value of c .

dimensional polynomial fit to those points yields an energy minimum for the values of a , b , and c as listed in Table I along with the results of our supplemental GPAW calculations.

The shallow minimum of the PBE total-energy curve at $c=4.87$ Å has the value 0.18 eV per unit cell compared to the layers taken apart, $c \rightarrow \infty$ ($c=4.89$ Å with 0.21 eV per unit cell for our GPAW calculations). This is in good agreement with the PW91 results of Ref. 12 where $c=4.84$ Å and a similar small surface energy in the cleavage plane was found. For truncated bulk they found the surface energy 0.048 J/m², approximately corresponding to a binding en-

ergy per unit cell of 0.25 eV. Our GGA results are also in good agreement with the PAW-based PBE results of Ref. 11. In all four GGA calculations, the value of the binding energy is unphysically small, illustrating the deficiency of GGA.

B. vdW-DF results

With vdW-DF we find total-energy curves (at fixed values of a and b) with enhanced binding compared to GGA (Fig. 3). The position of the minimum of the total-energy curve depends on our choice of GGA exchange, as discussed in the previous section. The optimal values of c and the binding energies for each choice of exchange functional are listed in Table I.

For vdW-DF with C09_x or PBEsol_x the value of c is close to the experimental value, in fact the optimal value of c with C09_x or PBEsol_x is 2% smaller than the experimental value. PBE_x and PW86_x, as recommended in Ref. 46, improve the binding over the results of GGA by decreasing c about 0.4 Å, resulting in a value of c that deviates from experiment by only 2%. The binding energies range from 0.86 eV/unit cell (for revPBE_x) to 1.48 eV/unit cell (PBEsol_x). As expected, revPBE_x leads to longer binding distances (8% larger than experiment) and a smaller binding energy than use of the other exchange forms because revPBE_x is overly repulsive.

In Table I we list two results based on revPBE_x. Previously, we have used the values of the revPBE_x energy that were provided from sc-GGA DACAPO calculations for input to the vdW-DF calculations. In this work we rely on our own external implementation for the exchange energy calculations. The implementation differences between DACAPO and our external code are minor and related to the choice of

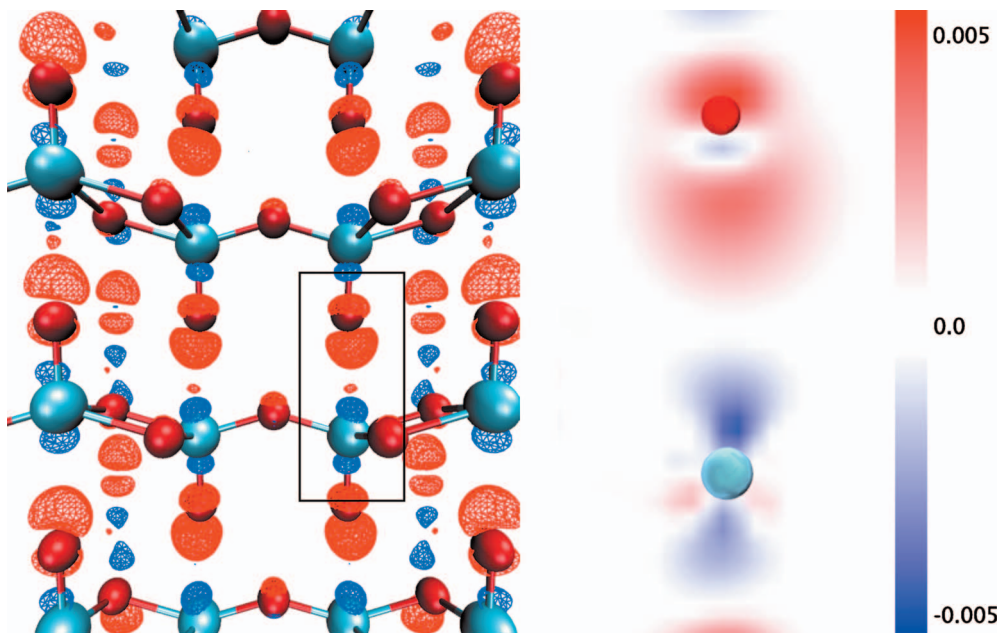


FIG. 4. (Color) Change in electron density, $\Delta n(\mathbf{r})$, as a result of assembling the layers of V₂O₅. Left: isosurfaces of values 0.02 $|e|/\text{Å}^3$ are shown, red indicates gain of electrons (loss of charge). The box indicates the region of the plot shown in the right panel. Right: the electron density difference is shown in a slice through the system, through the positions of the V atom and the corresponding vanadyl O atom of the next layer. Color scales are indicated in the right-hand bar, in units of $|e|/\text{Å}^3$. Figure created with VMD (Ref. 50).

numerical method for calculating the gradient ∇n , both are standard numerical library methods. As shown in Fig. 3 for revPBE_x, the differences in the numerical results are small and can be ignored.

While the discussion of best and physically most reasonable choice of exchange to go with vdW-DF is still open, it is clear from our total-energy calculations that the vdW forces do indeed play a prominent role in the binding of the V₂O₅ layers. Earlier, another group¹⁹ has examined the role of the vdW forces in V₂O₅ by means of the semiempirical DFT-D approach (Ref. 18), arriving at a similar conclusion.

The vdW-DF total-energy curves in Fig. 3 have small wiggles, in particular, in the expansion region ($c > 4.6$ Å). We find that the wiggles mainly arise from the exchange part of the energy, as also seen in, e.g., Refs. 37 and 47. The minimum of the $E^{\text{vdW-DF}}$ curves is found by a polynomial fit to the points closest to the minimum. From this fit we also extract the corresponding values of the elastic coefficient C_{33} (Table I). Because V₂O₅ is more soft (easier to expand or compress) in the direction perpendicular to the layers, compared to other directions, the value of C_{33} is also a good estimate of the bulk modulus of the system. Based on the likely most realistic exchange choices (i.e., excluding here the overly repulsive revPBE_x) we find that V₂O₅ bulk with $C_{33} \approx 60$ GPa is a somewhat more stiff material than graphite, which has⁴⁸ $C_{33} = 37\text{--}41$ GPa.

As seen in Table I, LDA gives fair numerical agreement for the V₂O₅ structure. However, these values are produced via an unphysical error cancellation. As discussed in several other publications (e.g., Refs. 17 and 26), for planar systems LDA is at best modeling the vdW binding. LDA lacks a physical description of the dispersive interactions and has no basis for a transferable account in more general geometries.¹⁷ In other geometries the LDA approach gives results that are not in accordance with experiment or more accurate methods.^{26,49}

C. Numerical noise and exchange functionals

Our DFT calculations are based on a description of the valence-electron wave functions by USPP. The USPP are not norm conserving and tend to give “noise” in regions of very low electron density, yielding some small (unphysical) negative values of n . In order to handle these small negative values of n , DACAPO replaces on the FFT grid points all values $n < n_{\text{floor,dac}}$ by $n_{\text{floor,dac}}$ before calculating the exchange energy. The floor is given in terms of the Bohr radius a_0 , $n_{\text{floor,dac}} = 10^{-10} |e|/a_0^3 \approx 10^{-9} |e|/\text{Å}^3$ being a small but positive minimum value of the density.

Points in space in which this floor is applied become, via the formula $s \sim |\nabla n|/n^{4/3}$, points with extremely large (unphysical) values of s . For exchange choices such as PBE_x and revPBE_x with a constant asymptote of $F_x(s)$ the effect of this replacement is small: very large values of s (≥ 100) contribute much less to the energy integral, Eq. (5), than do moderate values of s ($\approx 5\text{--}10$), because $F_x(s)$ is basically constant at large s (small n) and the integrand $n^{4/3} F_x$ thus vanishes for small n . However, for more “aggressive” exchange functionals, in terms of growth of F_x for large values

of s , this may cause problems in material systems with large regions of small or vanishing electron density (vacuum), such as our reference calculations. This is further discussed in two forthcoming publications.³⁸ Here, we simply state that the modification used in our external implementation is to instead *remove* contributions to the integral of Eq. (5) that come from points in space with $n < n_{\text{floor}} = 10^{-15} |e|/\text{Å}^3$, and that the procedure is not very sensitive to the particular value of n_{floor} .

We note that while we here show numerical problems encountered using USPP with the DFT code DACAPO some other DFT codes may face similar problems at various levels. Most DFT codes were not written with sparse systems and small energies in mind and we recommend an explicit test of effects of numerical noise with vdW-DF calculations.

At the time when dense, bulklike systems were the main systems examined with DFT, relevant values of s were considered to be small, in the approximate range²⁸ $0 < s < 3$. In sparse matter this is not always the case: in our sparse matter systems we routinely work with (physical) values of s which are several orders of magnitude larger than this. In our V₂O₅ reference calculations, consisting of a single layer of V₂O₅ surrounded by vacuum, almost 50% of the spatial grid points give rise to s values larger than 12 both in our USPP-based electron density from the DACAPO calculations and in the pseudopotential of the electron density of our supplemental GPAW calculations. In comparison, the bulk calculations at close-to-experimental separation ($c = 4.3$ Å) show mostly small values of s . We find that $s = 2.7$ is the largest value in the GPAW calculation for bulk V₂O₅ while only 0.4% of spatial points have large values ($s > 12$) in the corresponding DACAPO calculation.

As a measure of the effect of removing all points with $n < n_{\text{floor}}$ (including points with negative values of n) we calculate an error measure η . This error measure is defined as the (absolute value of the) contributions that would have come from the excluded points, weighted with the unit-cell size $V = abc$,

$$\eta = \frac{1}{V} \Delta \int_{n < n_{\text{floor}}} d\mathbf{r} |n| \epsilon_x^{\text{LDA}}(|n|) F_x \left(c_s \frac{|\nabla n|}{|n|^{4/3}} \right), \quad (6)$$

where the difference indicated by Δ is between contributions from bulk and reference calculations. We find that for each choice of exchange form this measure is approximately constant over the range of layer separations studied here with values ranging from $0.5 \text{ meV}/\text{Å}^3$ for C09_x to $1.0 \text{ meV}/\text{Å}^3$ for PW86_x. The fact that η is approximately constant with c fits well with our expectation that spatial points with $n < n_{\text{floor}}$ appear in the vacuum region of the unit cell in the reference calculations, a region that expands approximately as fast as V .

We note that the numerical problems faced here are similar to those one of us has previously documented for a molecular dimer.⁴⁷ Then, as part of an early vdW-DF study, we investigated the energy difference between a far-apart benzene dimer in a unit cell of a certain (large) size and two isolated benzene molecules each in a unit cell of the same size as the original unit cell. Whereas physically this energy

difference should vanish, a small but finite contribution δE_{ref} appeared.⁴⁷ This unphysical difference δE_{ref} would not converge with, e.g., plane-wave energy cutoff or other convergence parameters and it was found to originate mainly from the exchange part of the energy. In dimer and adsorption studies this problem can be overcome by simple error cancellation using a fixed size of the unit cell and moving the material fragments around.^{34,47} In bulk calculations the unit-cell size must necessarily change, and no such full error cancellation is possible, leading to a usually small but nonvanishing η .

D. Binding of layers

The results of our vdW-DF calculations, regardless of choice of exchange functional, indicate that the vdW forces are indeed important in the V_2O_5 system. We have further analyzed the system by extracting the change in electron density, $\Delta n(\mathbf{r})$, that arises when moving an isolated layer of V_2O_5 into the bulk structure (atom positions kept fixed). This short qualitative analysis is based on the $n(\mathbf{r})$ extracted from the sc-GGA calculations but we expect no major deviations from the result of using an electron density based on sc vdW-DF calculations.

Figure 4 shows that only a small amount of electron charge is moved when the V_2O_5 layers bind. Most of this change is on the vanadyl O atom and the V atom. A Bader analysis,⁵¹ using the algorithm described in Ref. 52 and discussed in Ref. 53, confirms this picture of very little change in charge: only about 0.1 electrons move from V to vanadyl O, the charge on all other atoms is almost unchanged. This is in agreement with results of Ref. 54.

We agree that the static electron density $n(\mathbf{r})$ may not be the best tool to interpret the binding character, as suggested and discussed in Ref. 55. Nevertheless, we believe that qualitatively the combined interpretation from Fig. 4 and from the

Bader analysis is sufficient to conclude that no short-range binding type (such as ionic or covalent bonds) can explain the main part of the binding of the V_2O_5 layers. We find that inclusion of dispersive interaction is essential to complete the description of V_2O_5 cohesion.

V. SUMMARY

In this paper we have studied the role of the van der Waals bonding inside a layered oxide by means of the (by now) well-tested vdW-DF method.^{20,21} In particular, we have underlined the importance of accounting for the long-range interactions that characterize this bonding in order to recover a structure of V_2O_5 close to that found by experiments. We have shown that the choice of exchange functional for the vdW-DF calculations can give noticeable differences in calculated binding distances and energies and the definition of the most appropriate exchange functional is still a matter of debate. Specifically, in this paper we have tested three promising functionals to be used with vdW-DF: PBEsol_x, C09_x, and PW86_x. We have also analyzed effects of numerical noise that may arise in studying sparse matter within DFT. This is important because there are large regions with low density, regions that may cause errors in the evaluation of exchange. Finally, we have identified how this error varies with the choice of exchange.

ACKNOWLEDGMENTS

We thank M. V. Ganduglia-Pirovano for introducing us to the problem of describing V_2O_5 with DFT and for constructive discussions. We also thank J. Rohrer, K. Berland, and P. Hyldgaard for valuable discussions of exchange functional issues. Partial support from the Swedish Research Council (VR) is gratefully acknowledged, as well as allocation of computer time at UNICC/C3SE (Chalmers) and SNIC (Swedish National Infrastructure for Computing).

*Corresponding author; schroder@chalmers.se

¹B. M. Weckhuysen and D. E. Keller, *Catal. Today* **78**, 25 (2003), and references therein.

²C. Julien, E. Haro-Poniatowski, M. A. Camacho-López, L. Escobar-Alarcón, and J. Jiménez-Jarquín, *Mater. Sci. Eng., B* **65**, 170 (1999).

³M. B. Sahana, C. Sudakar, C. Thapa, G. Lawes, V. M. Naik, R. J. Baird, G. W. Auner, R. Naik, and K. R. Padmanabhan, *Mater. Sci. Eng., B* **143**, 42 (2007).

⁴S.-L. Chou, J.-Z. Wang, J.-Z. Sun, D. Wexler, M. Forsyth, H.-K. Liu, D. R. MacFarlane, and S.-X. Dou, *Chem. Mater.* **20**, 7044 (2008).

⁵J. S. Braithwaite, C. R. A. Catlow, J. D. Gale, and J. H. Harding, *Chem. Mater.* **11**, 1990 (1999).

⁶M. V. Ganduglia-Pirovano and J. Sauer, *J. Phys. Chem. B* **109**, 374 (2005).

⁷T. Reeswinkel, D. Music, and J. M. Schneider, *J. Phys.: Condens. Matter* **21**, 145404 (2009).

⁸J. Goclon, R. Grybos, M. Witko, and J. Hafner, *J. Phys.: Con-*

dens. Matter **21**, 095008 (2009).

⁹Z. R. Xiao and G. Y. Guo, *J. Chem. Phys.* **130**, 214704 (2009).

¹⁰M. Willinger, N. Pinna, D. S. Su, and R. Schlögl, *Phys. Rev. B* **69**, 155114 (2004).

¹¹J. L. F. Da Silva, M. V. Ganduglia-Pirovano, and J. Sauer, *Phys. Rev. B* **76**, 125117 (2007).

¹²M. V. Ganduglia-Pirovano and J. Sauer, *Phys. Rev. B* **70**, 045422 (2004).

¹³G. Kresse, S. Surnev, M. G. Ramsey, and F. P. Netzer, *Surf. Sci.* **492**, 329 (2001).

¹⁴Z.-Y. Li and Q.-H. Wu, *J. Mater. Sci.: Mater. Electron.* **19**, S366 (2008).

¹⁵J. Goclon, R. Grybos, M. Witko, and J. Hafner, *Phys. Rev. B* **79**, 075439 (2009).

¹⁶P. Hejduk, M. Witko, and K. Hermann, *Top. Catal.* **52**, 1105 (2009).

¹⁷H. Rydberg, M. Dion, N. Jacobson, E. Schröder, P. Hyldgaard, S. I. Simak, D. C. Langreth, and B. I. Lundqvist, *Phys. Rev. Lett.* **91**, 126402 (2003).

- ¹⁸S. Grimme, *J. Comput. Chem.* **27**, 1787 (2006).
- ¹⁹T. Kerber, M. Sierka, and J. Sauer, *J. Comput. Chem.* **29**, 2088 (2008).
- ²⁰M. Dion, H. Rydberg, E. Schröder, D. C. Langreth, and B. I. Lundqvist, *Phys. Rev. Lett.* **92**, 246401 (2004); **95**, 109902(E) (2005).
- ²¹T. Thonhauser, V. R. Cooper, S. Li, A. Puzder, P. Hyldgaard, and D. C. Langreth, *Phys. Rev. B* **76**, 125112 (2007).
- ²²J. Kleis, E. Schröder, and P. Hyldgaard, *Phys. Rev. B* **77**, 205422 (2008).
- ²³K. Berland and P. Hyldgaard, *J. Chem. Phys.* **132**, 134705 (2010).
- ²⁴A. Kokalj, *Comput. Mater. Sci.* **28**, 155 (2003).
- ²⁵S. D. Chakarova-Käck, E. Schröder, B. I. Lundqvist, and D. C. Langreth, *Phys. Rev. Lett.* **96**, 146107 (2006).
- ²⁶J. Kleis, B. I. Lundqvist, D. C. Langreth, and E. Schröder, *Phys. Rev. B* **76**, 100201(R) (2007).
- ²⁷Open-source plane-wave DFT computer code DACAPO, <http://wiki.fysik.dtu.dk/dacapo/>
- ²⁸J. P. Perdew, K. Burke, and M. Ernzerhof, *Phys. Rev. Lett.* **77**, 3865 (1996); **78**, 1396(E) (1997).
- ²⁹Y. L. Kempf, B. Silvi, A. Dietrich, C. R. A. Catlow, and B. Maigret, *Chem. Mater.* **5**, 641 (1993).
- ³⁰E. Ziambaras, J. Kleis, E. Schröder, and P. Hyldgaard, *Phys. Rev. B* **76**, 155425 (2007).
- ³¹Open-source, grid-based PAW-method DFT code GPAW, <http://wiki.fysik.dtu.dk/gpaw/>
- ³²P. E. Blöchl, *Phys. Rev. B* **50**, 17953 (1994).
- ³³D. C. Langreth, M. Dion, H. Rydberg, E. Schröder, P. Hyldgaard, and B. I. Lundqvist, *Int. J. Quantum Chem.* **101**, 599 (2005).
- ³⁴S. D. Chakarova-Käck, A. Vojvodic, J. Kleis, P. Hyldgaard, and E. Schröder, *New J. Phys.* **12**, 013017 (2010).
- ³⁵Y. Zhang and W. Yang, *Phys. Rev. Lett.* **80**, 890 (1998).
- ³⁶D. C. Langreth, B. I. Lundqvist, S. D. Chakarova-Käck, V. R. Cooper, M. Dion, P. Hyldgaard, A. Kelkkanen, J. Kleis, L. Kong, S. Li, P. G. Moses, E. Murray, A. Puzder, H. Rydberg, E. Schröder, and T. Thonhauser, *J. Phys.: Condens. Matter* **21**, 084203 (2009).
- ³⁷Even though Hartree-Fock exchange, in principle, provides exact exchange, it is not a perfect alternative either, as discussed in, for example, Refs. 33, 42, and 46.
- ³⁸E. Londero and E. Schröder, [arXiv:1007.3045](https://arxiv.org/abs/1007.3045) (unpublished); K. Berland, Ø. Borck, and P. Hyldgaard, [arXiv:1007.3305](https://arxiv.org/abs/1007.3305) (unpublished).
- ³⁹J. P. Perdew, A. Ruzsinszky, G. I. Csonka, O. A. Vydrov, G. E. Scuseria, L. A. Constantin, X. Zhou, and K. Burke, *Phys. Rev. Lett.* **100**, 136406 (2008); **102**, 039902(E) (2009).
- ⁴⁰V. R. Cooper, *Phys. Rev. B* **81**, 161104(R) (2010).
- ⁴¹As defined in Ref. 56 with the refitted values given in Ref. 46.
- ⁴²J. P. Perdew, A. Ruzsinszky, J. Tao, V. N. Staroverov, G. E. Scuseria, and G. I. Csonka, *J. Chem. Phys.* **123**, 062201 (2005).
- ⁴³Y. Kanai and J. C. Grossman, *Phys. Rev. A* **80**, 032504 (2009).
- ⁴⁴R. Enjalbert and J. Galy, *Acta Crystallogr., Sect. C: Cryst. Struct. Commun.* **42**, 1467 (1986).
- ⁴⁵J. P. Perdew, in *Electronic Structure of Solids '91*, edited by P. Ziesche and H. Eschrig (Akademie Verlag, Berlin, 1991), p. 11; J. P. Perdew, J. A. Chevary, S. H. Vosko, K. A. Jackson, M. R. Pederson, D. J. Singh, and C. Fiolhais, *Phys. Rev. B* **46**, 6671 (1992); *Phys. Rev. B* **48**, 4978(E) (1993).
- ⁴⁶É. D. Murray, K. Lee, and D. C. Langreth, *J. Chem. Theory Comput.* **5**, 2754 (2009).
- ⁴⁷S. D. Chakarova and E. Schröder, *Mater. Sci. Eng., C* **25**, 787 (2005).
- ⁴⁸*Landolt-Börnstein Search* (Springer-Verlag, Berlin, 2003), <http://link.springer.de>.
- ⁴⁹M. S. Miao, M.-L. Zhang, V. E. Van Doren, C. Van Alsenoy, and J. L. Martins, *J. Chem. Phys.* **115**, 11317 (2001).
- ⁵⁰W. Humphrey, A. Dalke, and K. Schulten, *J. Mol. Graphics* **14**, 33 (1996).
- ⁵¹R. F. W. Bader, *Atoms in Molecules: A Quantum Theory* (Oxford University Press, Oxford, 1990).
- ⁵²G. Henkelman, A. Arnaldsson, and H. Jónsson, *Comput. Mater. Sci.* **36**, 354 (2006).
- ⁵³Ø. Borck and E. Schröder, *J. Phys.: Condens. Matter* **18**, 10751 (2006).
- ⁵⁴S. Laubach, P. C. Schmidt, A. Thißen, F. J. Fernandez-Madrigal, Q.-H. Wu, W. Jaegermann, M. Klemm, and S. Horn, *Phys. Chem. Chem. Phys.* **9**, 2564 (2007).
- ⁵⁵S. Nordholm and W. Eek, *Int. J. Quantum Chem.* (to be published).
- ⁵⁶J. P. Perdew and Y. Wang, *Phys. Rev. B* **33**, 8800(R) (1986).